Sociedade Brasileira de Automática (SBA)
XXIV Congresso Brasileiro de Automática - CBA 2022, 16 a 19 de outubro de 2022

# Robust Regional ISS Stabilization of Saturating State-Delayed Discrete-Time Systems ⋆

**Romulo J. Silva Jr.** * **Valter J. S. Leite** *,** **Luís F. P. Silva** **

* *Graduate Program on Electrical Engineering (PPGEL), CEFET-MG, Belo Horizonte, MG, Brazil,* 30510-000. *e-mail: romulojsj94@gmail.com*
** *Department of Mechatronics Engineering, CEFET-MG - Campus Divinópolis, Divinópolis, MG, Brazil,* 35503-822. *e-mails: valter@ieee.org, luis@cefetmg.br*

**Abstract:** Recent works in the literature deal with efficient numerical conditions to robustly stabilize state-delayed discrete-time systems under saturating actuators. However, practical issues such as the rejection of exogenous signals and their effects on the region of safe initial conditions have not been thoroughly investigated. This work extends a previous controller design condition to handle the $\ell_2$ gain between the exogenous signals and the measured output. Moreover, the notion of input-to-state stability is applied, allowing to consider the effects of the disturbance signals over the estimates of the safe initial conditions region. Furthermore, a recent optimization procedure formulated in an augmented space is applied, allowing better estimates of the region of safe initial conditions while maintaining the numerical complexity acceptable. A numerical example illustrate the methods proposed and compare the achievements with the concerned literature.

*Keywords:* Time-varying discrete-time systems, time-varying state-delays, saturating actuators, $\ell_2$-gain, Input-to-state stability, robust control.

## 1. INTRODUCTION

Practical processes usually have time-varying delays, saturating actuators, and exogenous signals that adversely affect performance or even stability (Fridman, 2014). State-delays are present in several applications such as power electronics and systems, aerospace engineering, electric circuit network, economics, and biological systems (MacDonald, 2008; Hu and Wang, 2013; Fu and Ma, 2016), representing a relevant challenge to both applications and theoretical tools. Moreover, real-world applications are subject to energy constraints and uncertainties on parameters, leading to loss of performance and even instability. Another issue is the presence of disturbance signals, causing state trajectories to deviate from the equilibrium condition.

Delayed discrete-time systems under saturating actuators have attracted attention in recent years. The works (Castro et al., 2020; Silva et al., 2018a; Chen et al., 2014) propose asymptotical stabilization conditions. Also, these works provide estimates for the set of initial conditions such that the closed-loop trajectories converge to the origin, i.e., estimates of the region of attraction. While (Castro et al., 2020) and (Chen et al., 2014) use a Lyapunov-Krasovskii (L-K) based approach, Silva et al. (2018a) adopt an augmented delay-free representation yielding much larger estimates of the region of attraction at a higher computational demand. However, disturbance signals are not concerned by any of the works mentioned above.

The use of local (regional) input-to-state stability (or stabilization) to handle delayed discrete-time systems founds in (De Souza et al., 2019) an approach based on augmented space, extending the results in (Silva et al., 2018a) to take into account the presence of exogenous signals. Therefore, such an approach heritages the computational demand verified in the latter. Inspired by the approach from De Souza et al. (2019) and Silva et al. (2018a), the authors in (Alves Lima et al., 2021) map the a Lyapunov-Krasovskii function into an augmented space to explore better optimization methods to enlarge the estimate region of attraction in the (local) robust stability analysis case. The advantage in this case is that the LMI conditions for designing the controller remains with numerical complexity independent of the maximum delay, $\bar{d}$. This very same idea was developed independently in (Silva Jr. et al., 2022) for a different Lyapunov-Krasovskii functional. However, only the precisely known case is addressed in (Alves Lima et al., 2021).

In (Pepe et al., 2017) and (Xu et al., 2012) the L-K functional based approach is employed, leading to ISS conditions. In special, Pepe et al. (2017) analyze incremental input-state stability in local and global exponential stability contexts of a class of nonlinear state delayed discrete-time systems. Despite the general formulation, it is not directly applied to saturating actuators case.

Our main contribution is twofold: firstly, we extend the recent contribution presented by Castro et al. (2020) to

⋆ V. J. S. Leite thanks the Brazilian agency CNPq for the partial support to this work under grant 311208/2019-3.

cope with input-to-state stabilization. Consequently, our approach provides convex conditions handling the $\ell_2$ gain between the measured output and the disturbance input signal. Secondly, we provide an optimization procedure achieving more significant estimates of the region of attraction. Despite using an L-K-based approach, the proposed optimization uses an enlarged space. Consequently, our proposal benefits from the L-K approach's lower numerical complexity while heritages better optimization conditions from the augmented space one. We formulate three optimization procedures to maximize the tolerable disturbance energy, maximize the set of initial conditions, and minimize the $\ell_2$ gain between the measured output and the disturbance input. Differently from the proposal in (Alves Lima et al., 2021), our approach allows handling uncertain systems, providing the synthesis of the (local) robust stabilizing control gain. Moreover, our approach uses a different Lyapunov-Krasovskii functional from the one employed in Alves Lima et al. (2021), extending the results in Castro et al. (2020). A numerical example provides comparisons with literature results, illustrating the efficiency and improvements of our proposal.

In the next section we present the problem formulation and in the Section 3 some preliminaries results are recalled. We give new input-to-state stabilization conditions in Section 4. Section 5 presents a numerical example illustrating this work's contributions, and the conclusions are given in Section 6.

*Notations:* Sets $\mathbb{N}$, $\mathbb{R}$, $\mathbb{R}^n$, and $\mathbb{R}^{n\times m}$ denote, respectively, the sets of positive integers, real numbers, real $n$-dimensional vectors, real matrices of dimensions $n \times m$, and real square symmetric positive semi-definite matrices of dimensions $n \times n$. For any integers $a \leq b$, notation $\mathcal{I}[a, b]$ stands for $[a, b] \cap \mathbb{N}$. Matrices $I$ and $0$ refers to as the identity and null matrices of appropriate dimensions, respectively. $M \in \mathbb{R}^{n\times m}$ and $x \in \mathbb{R}^n$ are, respectively, a matrix with dimensions $n \times m$ and the $n$-dimensional vector, both with real entries. The transpose of $M$ is noted by $M^\top$, $M_{(i)}$ ($M_{ii}$) means the $i$-th row (diagonal element $(i, i)$ of $M$. For sake of clarity, $M_{(i)}^\top$ stands for $(M_{(i)})^\top$, $\mathtt{tr}(M)$ for the trace of $M$, and $\mathtt{diag}\{M_1, M_2\}$ for the block diagonal matrix $\left[\begin{smallmatrix} M_1 & 0 \\ 0 & M_2 \end{smallmatrix}\right]$. The Euclidean norm of $x$ is denoted by $\|x\|$. The symbol $\star$ represents the symmetric transposed blocks in square matrices. The Kronecker product is denoted by $\otimes$. For a square matrix $M$, $\mathtt{He}(M) = M + M^\top$.

## 2. PROBLEM FORMULATION

Consider the discrete-time and uncertain system with time-varying delay in the states and subject to saturating inputs and limited energy disturbances given by:

$$\begin{cases} x_{k+1} &= Ax_k + A_d x_{k-d_k} + B\mathtt{sat}\left(u_k\right) + B_w w_k, \\ z_k &= Cx_k \\ x_{-j} &= \varphi_0(j), \quad \forall j \in \mathcal{I}[0, \bar{d}], \end{cases} \tag{1}$$

where $x_k \in \mathbb{R}^n$ is the states vector, $z_k \in \mathbb{R}^{n_z}$ is the regulated output, $u_k \in \mathbb{R}^{n_u}$ is the control signal, and $w_k \in \mathbb{R}^{n_w}$ is the disturbance vector input, which belongs to the set of energy signals $W_s$ described as follows:

$$W_s = \left\{ w_k \in \mathbb{R}^{n_w} : \|w_k\|_2^2 \leq \delta^{-1} \right\}. \tag{2}$$

The symmetric decentralized vectorial saturation function $\mathtt{sat}\left(u_k\right)$ is such that

$$\mathtt{sat}\left(u_{k(\ell)}\right) = \mathtt{sign}(u_{k(\ell)}) \min\{|u_{k(\ell)}|, \bar{u}_{(\ell)}\}. \tag{3}$$

The uncertainties and time-invariant system's matrices have appropriated dimensions and belong to a convex polytope:

$$[A \ A_d \ B \ B_w \ C] = \sum_{i=1}^{N} \alpha_i \left[A_i \ A_{di} \ B_i \ B_{wi} \ C_i\right], \tag{4}$$

where the known matrices $A_i$, $A_{di}$, $B_i$, $B_{wi}$, and $C_i$, $i \in \mathcal{I}[1, N]$, are associated with the $N$ polytope's vertices, and the uncertain and time-invariant parameter $\alpha$ belongs to $\Gamma$,

$$\Gamma = \left\{ \alpha \in \mathbb{R}^N : \sum_{i=1}^{N} \alpha_i = 1, \alpha_i \geq 0, i \in \mathcal{I}[1, N] \right\}.$$

The time-varying state-delay $d_k$ belongs to $\mathcal{I}[\underline{d}, \bar{d}]$, with $\underline{d}$ and $\bar{d}$ representing its lower and upper limits, $0 < \underline{d} \leq \bar{d} < \infty$. The initial conditions are given by a sequence detonated by $\varphi_0$, where each element of $\varphi_0$ is a vector belonging to $\mathbb{R}^n$. Therefore, $\varphi_0$ is a sequence of $\bar{d} + 1$ vectors $x_j \in \mathbb{R}^n$, with $j \in \mathcal{I}[-\bar{d}, 0]$, being noted by $\varphi_0 = \{x_{-j}\}_{j\in\mathcal{I}[0,\bar{d}]}$, or equivalently, in a instant $k$ by $\varphi_k(j) = x_{k-j}$.

The control law proposed in this work to stabilize the system (1) is given by:

$$u_k = Kx_k, \tag{5}$$

where $K \in \mathbb{R}^{n_u\times n}$ is the control gain matrix. Note that, as used in (Silva et al., 2020, 2018b; Zhao et al., 2021; Ghrab et al., 2021), more complete control laws may be considered, where, (some) delayed values $x_{k-j}$, $j \in \mathcal{I}[1, \bar{d}]$ may be considered, for more details see (De Souza et al., 2019). Therefore, by using the state feedback control law (5) in the system (1), we obtain the following closed-loop system:

$$\begin{cases} x_{k+1} &= Ax_k + A_d x_{k-d_k} + B\mathtt{sat}\left(Kx_k\right) + B_w w_k, \\ z_k &= Cx_k \end{cases} \tag{6}$$

Because of saturating actuators, we cannot guarantee global stability for the systems treated in this paper if they are unstable in open-loop (Tarbouriech et al., 2011). Therefore, we need to deal with local stabilization, considering the region of attraction $\mathcal{R}_\mathcal{A}$. It is well known that the computation of such a region is not easy task in general (Tarbouriech et al., 2011). Therefore, an estimated region of attraction $\mathcal{R}_\mathcal{E} \subseteq \mathcal{R}_\mathcal{A}$ is computed instead. We present in this paper a new methodology to characterize the estimated region of attraction $\mathcal{R}_\mathcal{E}$ in the next section. Moreover, we need to consider the disturbance vector input effect in the local stability of the closed-loop system (6). Consequently, we need to work with the input-to-state stability (ISS). In the sequence, we present a definition for ISS adapted from (Silva et al., 2021).

*Definition 1.* Consider a positive scalar $\delta$ and any sequence $w_k \in W_s$. The uncertain closed-loop system (6) is said to be input-to-state stable (ISS) if for any $\varphi_0 \in \mathcal{R}_\mathcal{E}$ [1] the resulting state trajectories remain bounded in $\mathcal{R}_\mathcal{A}$, for all $k \geq 0$, and they go to origin when the sequence $w_k$ vanishes.

[1] We make an abuse of notation to mean that all elements of $\varphi_0$ belongs to the region $\mathcal{R}_\mathcal{E}$.

Next, we formulate the main problem dealt in this paper.

*Problem 1.* Assume the uncertain discrete-time system (1)-(4). Determine a robust state feedback control gain for (5) and provide an estimate $\mathcal{R}_{\mathcal{E}} \subseteq \mathcal{R}_{\mathcal{A}}$, such that the resulting uncertain closed-loop system (6) is ISS. Moreover, the designed controller must ensure a certain upper limit of the $\ell_2$ gain, denoted by $\gamma$, from the perturbation $w_k$ to the regulated output $z_k$, such that

$$\|z_k\|_2 \leq \gamma(\|w_k\|_2 + \mathcal{B}), \tag{7}$$

where the initial condition $\varphi_0$ yields the bias term $\mathcal{B} \geq 0$.

## 3. PRELIMINARY RESULTS

We deal with the saturating actuators by using the generalized sector condition as proposed by Gomes da Silva Jr. and Tarbouriech (2005). Based on the nonlinearity deadzone, $\phi(u_k)$, we can rewrite the saturation as:

$$\texttt{sat}\,(u_k) = u_k - \phi(u_k). \tag{8}$$

Therefore, by applying (8) in (6), we obtain:

$$\begin{cases} x_{k+1} = (A+BK)x_k + A_d x_{k-d_k} - B\phi(Kx_k) + B_w w_k, \\ z_k \quad\;\; = Cx_k \end{cases} \tag{9}$$

The next Lemma presents the generalized sector condition.

*Lemma 1.* For an auxiliary vector $\omega$ with limited saturation, $\bar{u}$, $\bar{x}_k \in \mathbb{S}$, the function $\phi(Kx_k)$ satisfies the inequality:

$$\phi(Kx_k)^\top \mathcal{T}[\phi(Kx_k) + \omega] \leq 0, \tag{10}$$

for any positive defined matrix $\mathcal{T} \in \mathbb{S}_+^m$ and

$$\mathbb{S} = \{x_k \in \mathbb{R}^n : |Kx_k - \omega| \leq \bar{u}\}. \tag{11}$$

The Lemma's proof is presented in (Tarbouriech et al., 2011).

In this paper, we work with the same Lyapunov-Krasoviskii's candidate function proposed by Castro et al. (2020), that is presented as follows:

$$V(\bar{x}_k) = V_1(x_k) + V_2(\bar{x}_k) + V_3(\bar{x}_k), \tag{12}$$

where,

$$V_1(x_k) = x_k^\top \bar{P} x_k, \tag{13}$$

$$V_2(\bar{x}_k) = \sum_{i=k-\underline{d}}^{k-1} x_i^\top \bar{Q}_1 x_i + \sum_{i=k-\bar{d}}^{k-\underline{d}-1} x_i^\top \bar{Q}_2 x_i, \tag{14}$$

$$V_3(\bar{x}_k) = \underline{d} \sum_{i=1-\underline{d}}^{0} \sum_{j=k+i}^{k} y_j^\top \bar{Z}_1 y_j + (\bar{d}-\underline{d}) \sum_{i=1-\bar{d}}^{-\underline{d}} \sum_{j=k+i}^{k} y_j^\top \bar{Z}_2 y_j, \tag{15}$$

with, $y_j = x_j - x_{j-1}$, and

$$\bar{x}_k = \begin{bmatrix} x_k^\top & x_{k-1}^\top & x_{k-2}^\top & \cdots & x_{k-\bar{d}}^\top \end{bmatrix}^\top. \tag{16}$$

Note that the sequence defined by $\varphi_k$ is equivalently represented by $\bar{x}_k$. Therefore, from now on, the initial sequence of the system may be noted by $\varphi_0$ or $\bar{x}_0$. This candidate function is a Lyapunov-Krasoviskii's (L-K) function, if the following statements are verified:

$$\left.\begin{array}{c} \beta_1\|\bar{x}_k\|^2 \leq V(\bar{x}_k) \leq \beta_2\|\bar{x}_k\|^2, \\ \Delta V(\bar{x}_k) = V(\bar{x}_{k+1}) - V(\bar{x}_k) \leq -\beta_3\|\bar{x}_k\|^2 \end{array}\right\} \tag{17}$$

with $\bar{x}_k \in \mathcal{R}_{\mathcal{E}} \subseteq \mathbb{R}^{n\bar{d}}$ and the $\mathcal{K}_\infty$-class functions $\beta_1\|\bar{x}_k\|^2$, $\beta_2\|\bar{x}_k\|^2$, and $\beta_3\|\bar{x}_k\|^2$.

We use the L-K candidate function to characterize the estimate region of attraction, $\mathcal{R}_{\mathcal{E}}$. This characterization is adapted from the methodology proposed in (Silva Jr. et al., 2022), such that, if $V(\bar{x}_k)$ is an L-K function, then we characterize the set $\mathcal{R}_{\mathcal{E}}$ as $\mathcal{L}_{\mathcal{V}}(\eta)$, where:

$$\mathcal{L}_{\mathcal{V}}(\eta) = \{\bar{x}_k \in \mathbb{R}^{n\bar{d}};\ \bar{x}_0^T \bar{M} \bar{x}_0 \leq \eta^{-1}\}, \tag{18}$$

with $\bar{M} = P_f + Q_{1f} + Q_{2f} + Z_{1f} + Z_{2f}$, $\bar{P}_f = v_1 v_1^\top \otimes \bar{P}$, $Q_{1f} = \left(\sum_{i=2}^{1+\underline{d}} v_i v_i^\top\right) \otimes \bar{Q}_1$, $Q_{2f} = \left(\sum_{i=\underline{d}+2}^{\bar{d}+1} v_i v_i^\top\right) \otimes \bar{Q}_2$, $D_1 = \underline{d} \sum_{i=1}^{\underline{d}} \sum_{j=1}^{\underline{d}} v_i v_j^\top d_{1ij} \otimes \bar{Z}_1$, $Z_{1f} = \texttt{diag}(D_1, \mathbf{0})$, $D_2 = \iota_1 \sum_{i=1}^{\iota_1} \sum_{j=1}^{\iota_1} v_i v_j^\top d_{2ij} \otimes \bar{Z}_2$, $D_3 = \iota_2 \sum_{i=1}^{\iota_2} \sum_{j=1}^{\iota_2} v_i v_j^\top d_{3ij} \otimes \bar{Z}_2$, $Z_{2f} = -\iota_1^2 \texttt{He}(v_{(\iota_2+1)} v_{\iota_2}^\top) \otimes \bar{Z}_2 + \texttt{diag}(D_3, D_2)$, $\iota_1 = (\bar{d} - \underline{d})$, $\iota_2 = (\underline{d}+1)$, $v_i = \begin{bmatrix} 0_{n(1\times i-1)n} & I_n & 0_{n(1\times \bar{d}+1-i)n} \end{bmatrix}$, and $d_{kij} = d_{kji}$, $k \in \{1,2,3\}$,

$$d_{1ij} = \begin{cases} \underline{d}, \ i = j = 1 \\ 2\underline{d} - (2i-3), \ i = j > 1 \\ -(\underline{d} - (i-2)), \ |i-j| = 1 \\ 0, \text{ otherwise} \end{cases}$$

$$d_{2ij} = \begin{cases} 2\iota_1 - (2i-1), \ i = j \\ -(\iota_1 - (i-1)), \ |i-j| = 1 \\ 0, \text{ otherwise} \end{cases}, \text{and}$$

$$d_{3ij} = \begin{cases} \iota_2, \ i = j = 1 \\ 2\iota_2, \ i = j > 1 \\ -\iota_2, \ |i-j| = 1 \\ 0, \text{ otherwise.} \end{cases}$$

*Remark 1.* It is worth to say that the level set definied in (18) belongs to a lifted space. Such a feature allows better optimization procedures whithout increasing the computational cost of the stabilization conditions (see next section).

The following Lemma shows the local ISS stability and it was adapted from (De Souza et al., 2019).

*Lemma 2.* Consider a L-K function $V(\bar{x}_k)$ and $w_k \in W_s$ for a given $\delta$. If for every $\bar{x}_0 \in \mathcal{L}_{\mathcal{V}}(\eta)$ for a $\gamma$,

$$\Delta V(\bar{x}_k) - w_k^\top w_k + \gamma^{-2} z_k^\top z_k < 0 \tag{19}$$

is verified along the trajectories of system (6), then

$$V(\bar{x}_k) - V(\bar{x}_0) - \sum_{i=0}^{k} w_i^\top w_i + \frac{1}{\gamma^2} \sum_{i=1}^{k} z_i^\top z_i < 0, \quad \forall k > 0. \tag{20}$$

Hence, $\forall \bar{x}_0 \in \mathcal{L}_{\mathcal{V}}(\eta)$ and $w_k \in W_s$, it follows that

(1) $V(\bar{x}_k) \leq \|w_k\|_2^2 + V(\bar{x}_0) \leq \delta^{-1} + \eta^{-1} = \mu^{-1}$, for all $k > 0$ and, thus, the trajectories of the system remain bounded in $\mathcal{L}_{\mathcal{V}}(\eta) \subseteq \mathcal{R}_{\mathcal{A}}$;
(2) For $k \to \infty$, $\|z_k\|_2^2 < \gamma^2\big(\|w_k\|_2^2 + V(\bar{x}_0)\big)$;
(3) If $w_k = \mathbf{0}$ for all $k \geq \bar{k} \geq 0$, then $\bar{x}_k \to \mathbf{0}$ without leaving $\mathcal{R}_{\mathcal{E}}$ as $k \to \infty$.

## 4. MAIN RESULTS

In this section, we propose the following Theorem, where we show a solution for the Problem 1.

*Theorem 1.* Consider the system (1) under the control law expressed in (5). If exist the symmetric positive definite matrices $W$, $Q_1$, $Q_2$, $Z_1$, and $Z_2$ with real entries and dimensions $n \times n$, $L \in \mathbb{R}^{m\times n}$, $G \in \mathbb{R}^{m\times 4n}$, the positive defined diagonal matrix $\mathcal{T} \in \mathbb{R}^m$, a scalar $\varepsilon \in [0,\ 2]$, and positive scalars $\eta$ and $\delta$, that satisfies the followings LMIs:

$$\begin{bmatrix} \left(\begin{bmatrix}\Theta_{1i} & 0\\ 0 & 0\end{bmatrix} + \mathrm{He}\left(F_1^\top \Phi_{3i}^\top\right) - F_6^\top F_6\right) & \begin{bmatrix}\Theta_{2i}\\ (B_{wi})^\top\end{bmatrix} & F_{ci}^\top \\ \star & \Theta_3 & 0 \\ \star & \star & -\gamma^2 I \end{bmatrix} < 0, \tag{21}$$

$$\forall i \in \mathcal{I}[1,N],$$

$$\begin{bmatrix} \begin{bmatrix} W & 0 \\ \star & \mathcal{Q}_1 \end{bmatrix} & ([L\ 0] - G)_{(\ell)}^\top \\ \star & \eta u_{0(\ell)}^2 \end{bmatrix} \geq 0, \tag{22}$$

$$\forall \ell \in \mathcal{I}[1, n_u],$$

where

$$\Theta_{1i} = \begin{pmatrix} \mathrm{He}\left(F_1^\top \Phi_{2i}^\top - F_5^\top G \Xi\right) \\ +\mathcal{Q}_2 - 2F_5^\top \mathcal{T} F_5 \\ -\Pi^\top \begin{bmatrix} Z_1 & 0 \\ \star & Z_2 \end{bmatrix} \Pi \end{pmatrix} \tag{23}$$

$$\Theta_{2i} = [A_i W + B_i L - W\ \ 0\ \ A_{di} W\ \ 0\ \ B_i \mathcal{T}]^\top, \tag{24}$$

$$\Theta_3 = \varepsilon^2(\underline{d}^2 Z_1 + (\bar{d} - \underline{d})^2 Z_2) - (2\varepsilon - \varepsilon^2) W, \tag{25}$$

with follow matrices

$$\mathcal{Q}_1 = \mathtt{diag}(Q_1, Q_2, Q_2), \tag{26}$$

$$\mathcal{Q}_2 = \mathtt{diag}(Q_1, -Q_1 + Q_2, 0, -Q_2, 0, 0), \tag{27}$$

$$\Pi = \begin{bmatrix} I & -I & 0 & 0 & 0 \\ 0 & I & -2I & I & 0 \end{bmatrix}, \quad \begin{matrix} F_1 = [I\ 0\ 0\ 0\ 0], \\ F_5 = [0\ 0\ 0\ 0\ I], \end{matrix} \tag{28}$$

$$\Xi = \begin{bmatrix} I & 0 & 0 & 0 & 0 \\ 0 & I & 0 & 0 & 0 \\ 0 & 0 & I & 0 & 0 \\ 0 & 0 & 0 & I & 0 \end{bmatrix}, \tag{29}$$

$$F_{ci} = F_1 \otimes C_i, \tag{30}$$

$$\Phi_{3i} = [0\ 0\ 0\ 0\ 0\ B_{wi}], \tag{31}$$

$$F_6 = [0\ 0\ 0\ 0\ 0\ I], \tag{32}$$

and, $\bar{P} = W^{-1}$, $\bar{Q}_1 = W^{-1} Q_1 W^{-1}$, $\bar{Q}_2 = W^{-1} Q_2 W^{-1}$, $\bar{Z}_1 = W^{-1} Z_1 W^{-1}$, $\bar{Z}_2 = W^{-1} Z_2 W^{-1}$. Then, the robust control gain can be obtained from

$$K = L W^{-1} \tag{33}$$

ensuring that the uncertain closed-loop system (9) is ISS. Moreover, for all $\bar{x}_0 \in \mathcal{L}_\mathcal{V}(\eta)$ and $w_k \in W_s$ the following statements are verified:

(1) $V(\bar{x}_k) \leq \|w_k\|_2^2 + V(\bar{x}_0) \leq \delta^{-1} + \eta^{-1} = \mu^{-1}$, for all $k > 0$ and, thus, the trajectories of the system remain bounded in $\mathcal{L}_\mathcal{V}(\eta) \subseteq \mathcal{R}_\mathcal{A}$;
(2) For $k \to \infty$, $\|z_k\|_2^2 < \gamma^2\big(\|w_k\|_2^2 + V(\bar{x}_0)\big)$;
(3) If $w_k = \mathbf{0}$ for all $k \geq \bar{k} \geq 0$, then $\bar{x}_k \to \mathbf{0}$ without leaving $\mathcal{R}_\mathcal{E}$ as $k \to \infty$.

*Proof :* If we take out the columns and rows six and eight in the LMIs (21) and if we consider $\eta = 1$ in (22), we recover the results presented in (Castro et al., 2020). Based on this and considering that LMIs (21) are verified, we get

$$\Delta V(\bar{x}_k) - \mathtt{He}(\phi(Kx_k)^\top \mathcal{T}(\phi(Kx_k) + \omega)) - w_k^\top w_k + \gamma^{-2} z_k^\top z_k < 0. \tag{34}$$

If $\bar{x}_k$ is such that the set $\mathbb{S}$ is verified, then the inequality (10) is true and, consequently, the inequality (19) is verified and the function (12) is a L-K function. Considering now that even (21), the LMIs (22) are verified, following (Castro et al., 2020), we can guarantee that $Kx_k \in \mathbb{S}$, the Lemma 2 is verified and, then, the resulting uncertain closed-loop system is ISS with the estimated region of attraction given by $\mathcal{L}_\mathcal{V}(\eta)$ in (18). ♢

*Remark 2.* A relevant factor for validating the efficiency of the proposed conditions is the analysis of numerical complexity, that depends on the number of scalar variables $\mathcal{K}$ and the number of rows $\mathcal{L}$, given by $\mathcal{L}_1 = N(4n+1+n)+2Nn+n+n_u(4n+1)$ and $\mathcal{K}_1 = n_u n + n^2 + \frac{5n(n+1)}{2} + 1$. Note that the numerical complexity does not depend on the delay variation, so it is significantly lower compared to an augmented system, as presented by (De Souza et al., 2019), shown below to comparison.

$$\begin{aligned} \mathcal{L}_c &= [2n(\bar{d}+1) + m + q + l]N\hat{t}[\hat{t}^2 - (\hat{t} - \Delta\tau_{\max}) \\ &\quad \times(\bar{d} - \Delta\tau_{\max} - 1)] + [n(\bar{d}+1)+1]N\hat{t}m\,, \\ \mathcal{K}_c &= 0.5n^2(\bar{d}+1)^2(N\hat{t}+2) \\ &\quad +0.5n(\bar{d}+1)N\hat{t} + m[2n(\bar{d}+1)+1] + 1. \end{aligned} \tag{35}$$

with $\hat{t} = (\bar{d} - \underline{d} + 1)$, and $\Delta\tau_{\max}$ the maximum delay interval.

### 4.1 Structures of the optimization procedures

We present three optimization procedures used to maximize the region of attraction, the disturbance tolerance maximization, and disturbance effects minimization.

(1) Minimizing the trace of $\mathcal{H}$: the objective is maximize the estimated region $\mathcal{R}_\mathcal{E}$, bringing it closer to the region of attraction $\mathcal{R}_\mathcal{A}$. In this case, $\forall k \geq 0$, the controller gains are calculated to determine this, for a system without disturbance, namely, $w_k = 0$. Futhermore $(M - \mathcal{W})^\top M^{-1}(M - \mathcal{W}) \geq 0$, or equivalently

$$0 < \bar{M} = \mathcal{W}^{-1} M \mathcal{W}^{-1} \leq (2\mathcal{W} - M)^{-1} \leq \mathcal{H}, \tag{36}$$

with

$$\begin{aligned} \mathcal{H} = \mathcal{H}^\top &\in \mathbb{R}^{(\bar{d}+1)n\times(\bar{d}+1)n} \\ \mathcal{W}^{-1} &= I_{\bar{d}+1} \otimes W^{-1}. \end{aligned} \tag{37}$$

Thus, we have,

$$\mathcal{J}_1 = \begin{cases} \min\limits_{\mathcal{H},\mathcal{W},M,L,G,\varepsilon,\mathcal{T},\eta,\gamma,\delta} & \mathtt{tr}\Big(\mathcal{H}\Big) \\ & (21), (22), \mathtt{and} \\ \mathtt{s.t.} & \begin{bmatrix} 2\mathcal{W} - M & I \\ I & \mathcal{H} \end{bmatrix} \succeq 0 \end{cases} \tag{38}$$

(2) Maximum tolerance to the disturbance $\delta^{-1}$: for null initial conditions, the admissible disturbance are maximized, therefore, $\delta^{-1}$ is the largest possible, if

the system is regulated $x_0 = 0$ then $\delta^{-1} = \eta^{-1}$. Therefore, for the optimization procedure, the value of $\gamma$ is fixed, thus analyzing the minimization of the $\delta$ factor for a given interval of $\overline{u}$.

$$\mathcal{J}_2 = \begin{cases} \min\limits_{\mathcal{H},\mathcal{W},M,L,G,\varepsilon,\mathcal{T},\eta} & \delta \\ \texttt{s.t.} & (21),(22), \\ & \text{and fixed } \gamma \end{cases} \tag{39}$$

(3) Minimizing disturbance effects: for a given perturbation energy, $\delta^{-1}$, to determine the robust gains of the controller, it is possible to minimize the gain $\ell_2$ between the disturbance and the regulated output of the system, analyzing thus, minimizing the factor $\gamma$ for a given interval of $\overline{u}$.

$$\mathcal{J}_3 = \begin{cases} \min\limits_{\mathcal{H},\mathcal{W},M,L,G,\varepsilon,\mathcal{T},\eta} & \gamma \\ \texttt{s.t.} & (21),(22), \\ & \text{and fixed } \delta \end{cases} \tag{40}$$

## 5. NUMERICAL EXAMPLE

We propose a numerical example to illustrate the main contributions of this work. Consider the discrete-time system (1) with time-delay in the states $d_k \in \mathcal{I}[2,4]$, saturating actuators, with $\overline{u} = 10$, and matrices:

$$A_1 = \begin{bmatrix} 0.38 & 0.2 \\ 0.09 & 1.00 \end{bmatrix}, \; A_{d_1} = \begin{bmatrix} 0.01 & -0.03 \\ 0.02 & 0 \end{bmatrix}, \; B_1 = \begin{bmatrix} 1.98 \\ 0.99 \end{bmatrix},$$
$$A_2 = \begin{bmatrix} 0.42 & 0.2 \\ 0.11 & 1.00 \end{bmatrix}, \; A_{d_2} = \begin{bmatrix} 0.05 & 0.09 \\ 0.04 & 0.06 \end{bmatrix}, \; B_2 = \begin{bmatrix} 2.02 \\ 1.01 \end{bmatrix},$$
$$B_{w_1} = \begin{bmatrix} 0.198 \\ 0.099 \end{bmatrix}, \; C_1 = \begin{bmatrix} 1 \\ 0 \end{bmatrix}^\top, B_{w_2} = \begin{bmatrix} 0.202 \\ 0.101 \end{bmatrix}, \; C_2 = \begin{bmatrix} 0 \\ 1 \end{bmatrix}^\top. \tag{41}$$

Firstly, we work with the maximization of the estimated region of attraction. Therefore, from the $\mathcal{J}_1$ optimization procedure, we can maximize the estimated region of attraction. We compare the regions of attraction sizes obtained from our results and the conditions proposed by Castro et al. (2020). Using our procedure, we choose $\epsilon$ equals 1.1, and using the procedure proposed in (Castro et al., 2020), we choose this variable equals 1.678. Our choice was based on the biggest obtained from the two optimization procedures in two cases. The following table presents the results obtained. We can see that the region of attraction

| Procedure | Radius | Volume |
|---|---|---|
| $\mathcal{J}_{1_{\varepsilon=1.1}}$ | 88.64 | $3.8570 \times 10^{24}$ |
| Castro et al. (2020)$_{\varepsilon=1.678}$ | 55.23 | $4.2028 \times 10^{23}$ |

Table 1. Comparison of the projected radius and volume of the estimated region of attraction.

radius obtained from our procedure results in 60.5% bigger than that obtained from the procedure proposed by Castro et al. (2020). Concerning the volume, our proposal achieves a size more than 9.3 bigger than the one by Castro et al. (2020). Such a comparison was performed by using the L-K matrices found by the approach in (Castro et al., 2020) and replacing them in the level set (18).

We present in Figure 1 the projection of the closed-loop system trajectories over $x_{k(1)} \times x_{k(2)}$ for 5 different initial

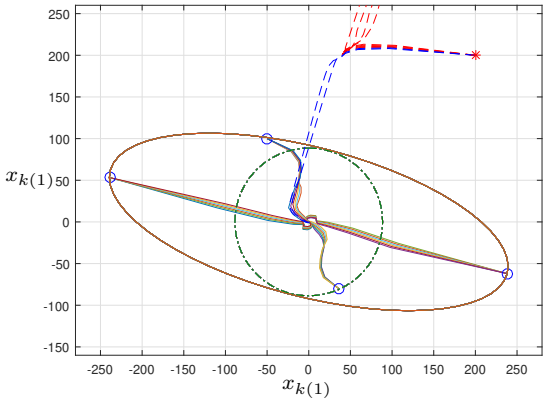


Figure 1. Convergence of initial conditions

conditions. For each initial condition a set of 6 simulations were performed, each of them with a different value of $\alpha_1 \in \{0, 0.2, 0.4, 0.6, 0.8, 1\}$. For each initial condition we took $x_{-j} = 0$, $j = 1, \ldots, 4$, and the values of $x_0$ are marked with in the plot with a $\circ$, yielding convergent trajectories, and with a $*$. In this last case, since the initial condition has been taken out of the estimated region of attraction, the convergence is not ensured. As one can see, 4 trajectories diverge from the origin (for $\alpha_1 \in \{0.4, 0.6, 0.8, 1\}$). The reader can note the green circle used to establish numerical comparison with other literature results, which demonstrates the superiority of our achievements.

Next, we use the optimization procedures $\mathcal{J}_2$ and $\mathcal{J}_3$ for the saturation value, $\bar{u}$, belongs to the interval [9.8, 15]. Considering the procedure $\mathcal{J}_2$, we verified the disturbance tolerance with $\gamma = 0.7071$ and $\gamma = 0.3873$. For the procedure $\mathcal{J}_3$, we analyzed for four cases, where $\delta = 2.8 \times 10^{-5}$, $\delta = 3.5 \times 10^{-5}$, $\delta = 4 \times 10^{-4}$, and $\delta = 2 \times 10^{-4}$. The Figure 2 summarizes the achievements as discussed in the sequel.

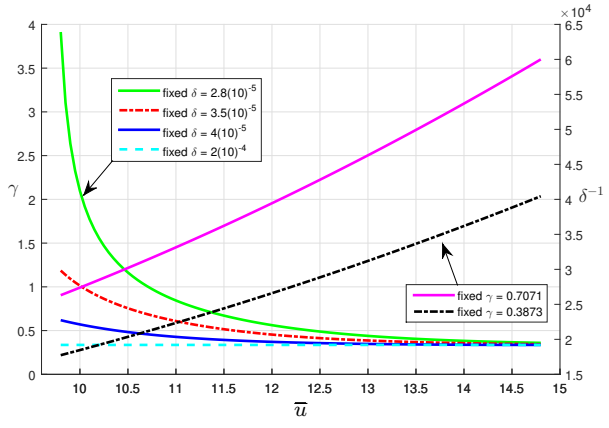


Figure 2. Relationship between the weighting of the $\ell_2$ gain for a fixed energy and, the maximum disturbance energy for a fixed $\gamma$, over each choice of $\overline{u}$.

By sweeping the control signal saturation limit, a relationship between the $\ell_2$ gain, $\gamma$, and the maximum disturbance energy, $\delta^{-1}$, can be obtained as shown in Fig. 2. By observing lines green, red, blue, and cyan, we note that bigger

values of $\bar{u}$, lead to a reduction of the $\ell_2$-gain, $\gamma$, which converges to the minimum value corresponding to 0.3362. Moreover, from this set of lines, we can see that the higher the tolerable energy, the higher the $\ell_2$-gain, meaning that the disturbance signal more influences the output. Such a behavior is more evident for lower values of $\bar{u}$.

Another numerical experiment was performed by fixing $\gamma$ and observing the maximal tolerable energy achieved with optimization procedure $\mathcal{J}_2$ for the assumed range of $\bar{u}$ (see magenta and black lines). In both cases, the tolerable disturbance energy grows with $\bar{u}$. Similarly to the previous experiment, we see that lower $\ell_2$-gains implies in lower values of disturbance energy.

Assuming a maximal disturbance energy $\delta^{-1} = 3.5714 \times 10^4$ and $\bar{u} = 10$, the optimization procedure $\mathcal{J}_3$ was used to design a robust state feedback control gain given by $K = [-0.0694 \ -0.2417]$. Then, we simulate the closed-loop (9) with a disturbance signal

$$w_k = [\mathbf{0}_{1,29} \ w_{30} \ w_{31} \ w_{32} \ \mathbf{0}_{1,28},] \tag{42}$$

with $w_{30} = \cos(\theta)\sqrt{\delta^{-1}}$, $w_{31} = \sqrt{\delta^{-1} - w_{30}^2 - w_{32}^2}$, $w_{32} = \sin(\theta)\sqrt{\delta^{-1}}$, and $\theta = \frac{\pi}{4}$, guaranteeing a signal of disturbance with maximum energy ($\delta^{-1} = 3.5714 \times 10^4$), applied from $k = 30$ up to $k = 32$. The initial condition $\varphi_0 = \left\{ \begin{bmatrix} -70 \\ -70 \end{bmatrix}, \begin{bmatrix} 31 \\ 50 \end{bmatrix}, \begin{bmatrix} 5 \\ 50 \end{bmatrix}, \begin{bmatrix} 38 \\ 25 \end{bmatrix}, \begin{bmatrix} 5 \\ 60 \end{bmatrix} \right\}$ belonging to $\mathcal{R}_\mathcal{E}$ was used. Figure 3 shows the behaviors of the states and control signal. Observe in the bottom subplot the saturation of the control signal in the first 4 or 5 samples and that, despite not achieving the saturation limit, the control signal can mitigate the disturbance signal. In all simulations, the delay was constant and equal to 4. All simulations were repeated under equal conditions for $\alpha_1 \in \{0, 0.2, 0.4, 0.6, 0.8, 1\}$.

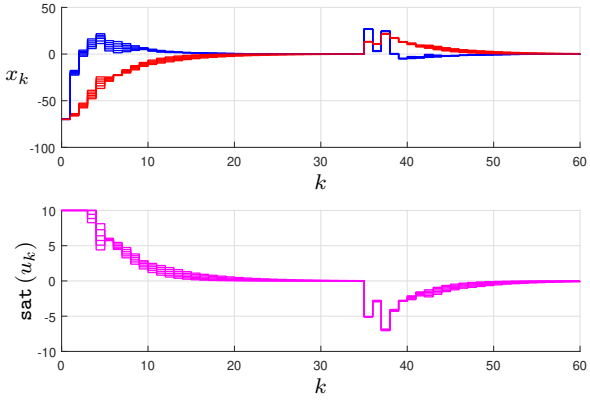


Figure 3. Convergence of states and saturated control signal for the configuration of the first vertex of the system.

## 6. CONCLUSIONS

The conditions proposed in the present work extend previous results from the literature to handle the robust input-to-state stabilization of discrete-time state delayed systems under saturating actuators and energy disturbance signals. Three optimization procedures were proposed, allowing the maximization of the tolerable disturbance energy, the maximization of the estimate of the region of attraction, or the minimization of the $\ell_2$-gain between the measured output and the disturbance signal. Furthermore, our approach's key feature consists of performing the optimization in a lifted space while keeping simple Lyapunov-Krasovskii candidate functions. Consequently, we can achieve better results at the expanse of low increase in the computational complexity. An example was proposed to compare our achievements with other results from the literature and illustrate the proposal's application. In future research, we may consider the multiobjective optimization problem, determining in the feasible objective space a subset of solutions close to the Pareto-optimal frontier, thus relating the three proposed convex optimization problems. Also, the time-varying parameter case deserves attention, providing controller design solutions to the (quasi-)LPV case.

## REFERENCES

Alves Lima, T., Tarbouriech, S., Gouaisbaut, F., Almeida Filho, M. P., García, P., Claure Torrico, B., and Gonzalez Nogueira, F. (2021). Analysis and experimental application of a dead-time compensator for input saturated processes with output time-varying delays. IET Control Theory and Applications, 15(4), 580–593.

Castro, M.F.F., Seuret, A., Leite, V.J.S., and Silva, L.F.P. (2020). Robust local stabilization of discrete time-varying delayed state systems under saturating actuators. Automatica, 122, 109266.

Chen, Y., Fei, S., and Zhang, K. (2014). Stabilisation for switched linear systems with time-varying delay and input saturation. International Journal of Systems Science, 45(3), 532–546.

De Souza, C., Leite, V.J.S., Silva, L.F.P., and Castelan, E.B. (2019). ISS robust stabilization of state-delayed discrete-time systems with bounded delay variation and saturating actuators. IEEE Transactions on Automatic Control, 64, 3913 – 3919.

Fridman, E. (2014). Introduction to Time-Delay Systems. Systems & Control: Foundations & Applications. Birkhäuser.

Fu, L. and Ma, Y. (2016). Passive control for singular time-delay system with actuator saturation. Applied Mathematics and Computation, 289, 181–193.

Ghrab, S., Benamor, A., and Messaoud, H. (2021). A new robust discrete-time sliding mode control design for systems with time-varying delays on state and input and unknown unmatched parameter uncertainties. Mathematics and Computers in Simulation, 190, 921–945.

Gomes da Silva Jr., J.M. and Tarbouriech, S. (2005). Antiwindup design with guaranteed regions of stability: an LMI-based approach. IEEE Transactions on Automatic Control, 50(1), 106–111.

Hu, H.Y. and Wang, Z.H. (2013). Dynamics of controlled mechanical systems with delayed feedback. Springer Science & Business Media.

MacDonald, N. (2008). Biological delay systems: linear stability theory. Cambridge University Press.

Pepe, P., Pola, G., and Di Benedetto, M.D. (2017). On Lyapunov-Krasovskii characterizations of stability notions for discrete-time systems with uncertain time-

varying time delays. IEEE Transactions on Automatic Control, 63(6), 1603–1617.

Silva, J.V.V., Silva, L.F.P., Rubio Scola, I., and Leite, V.J.S. (2018a). Robust local stabilization of discrete-time systems with time-varying state delay and saturating actuators. Mathematical Problems in Engineering, 2018.

Silva, L. F. P. , Leite, V. J. S., Castelan, E. B., and de Souza, C. (2021). Regional input-to-state stabilization of fuzzy state-delayed discrete-time systems with saturating actuators. Information Sciences, 557, 250–267.

Silva, L. F. P., Leite, V. J. S., Castelan, E. B., and Feng, G. (2018b). Delay dependent local stabilization conditions for time-delay nonlinear discrete-time systems using Takagi-Sugeno model. Int. J. Control Autom. Syst., 16, 1435–14475.

Silva, L. F. P., Leite, V. J. S., Castelan, E. B., Klug, M., and Guelton, K. (2020). Local stabilization of nonlinear discrete-time systems with time-varying delay in the states and saturating actuators. Information Sciences, 518, 272–285.

Silva Jr., R. J., Leite, V. J. S., and Silva, L. F. P. (2022). Proceedings of the 15th APCA International Conference on Automatic Control and Soft Computing, chapter A General Optimization Approach to Enlarge the Region of Attraction of Saturating Discrete-Time Delayed Systems, 1–10. Lecture Notes in Electrical Engineering. Springer Cham, Caparica, PT. To appear.

Tarbouriech, S., Garcia, G., Gomes da Silva Jr., J. M., and Queinnec, I. (2011). Stability and stabilization of linear systems with saturating actuators. Springer Science & Business Media.

Xu, S., Feng, G., Zou, Y., and Huang, J. (2012). Robust controller design of uncertain discrete time-delay systems with input saturation and disturbances. IEEE Transactions on Automatic Control, 57(10), 2604–2609.

Zhao, Y., Liu, Y., and Ma, Y. (2021). Robust finite-time sliding mode control for discrete-time singular system with time-varying delays. Journal of the Franklin Institute, 358(9), 4848–4863.